Available online at www.sciencedirect.com

ScienceDirect

Procedia Engineering 103 (2015) 52 – 59

Procedia Engineering

www.elsevier.com/locate/procedia

The 13th Hypervelocity Impact Symposium

Guided Impact Mitigation in 2D and 3D Granular Crystals

Hayden A. Burgoyne[a], John A. Newman[b], Wade C. Jackson[b], Chiara Daraio[c,a]*

[a]*Caltech, 1200 E. California Blvd, Pasadena, CA, 91125, USA*
[b]*NASA Langley Research Center, Hampton, VA, 23666, USA*
[c]*ETH Zurich, Tannenstrasse 3, Zurich, 8092, Switzerland*

Abstract

We simulate the dynamics of impacts on 1D, 2D and 3D arrays of metallic spheres in order to design novel granular protection systems. The dynamics of these highly organized systems of spheres, commonly called granular crystals, are governed by the contact law that describes how each particle interacts with the others. We use our recently developed force-displacement model of the dynamic compression of elastic-plastic spheres as the building block to investigate the response of systems comprised of metallic spheres to an impact. We first provide preliminary experimental results using a drop tower as validation of our numerical approach for 2D and 3D systems. We then use simulations of large periodic granular crystals in order to determine which particle properties govern the velocity of stress waves in these materials. We show that the properties of 1D systems can be scaled to predict the behavior of more complex 2D and 3D granular crystals. Because we can choose the material properties of each of the constituent particles and design how the particles are geometrically packed, we can leverage the heterogeneity of the system to create materials with unique properties such as anisotropic local stiffnesses and wave propagation velocities. We show that these materials allow us to design the dispersion and dissipation properties within the material in order to influence the propagation of a stress wave. Using these materials, we can therefore design protection systems or armor that directs damage away from sensitive parts or localizes damage to an unimportant area after impact from a projectile or a blast.

Peer-review under responsibility of the Curators of the University of Missouri On behalf of the Missouri University of Science and Technology
Keywords: granular, impact protection, wave speed, dispersion, dissipation, metamaterials

1. Introduction

Granular materials, such as sand and gravel, are often used as impact absorbers to protect from blasts, projectiles and shrapnel. Energy is dissipated by consolidation and rearrangement of grains, as well as by crushing and fracture at the contacts between grains [1]. A typical granular material consists of a random packing of grains of many sizes, shapes and potentially different material properties. In bulk granular materials, dispersion and dissipation properties are homogenized and nearly isotropic when the length scales of interest are much larger than the length scale of the individual random grains (as is typically the case). However, in more ordered states, granular materials can also consist of highly packed, periodic arrangements of uniform spherical particles, generally referred to as "granular crystals" [2]. These organized systems have been recently shown to allow choices of geometrical arrangement and material properties of constituent particles to control the wave propagation properties in the bulk [3-7]. Extensive experiments and simulations have been performed on granular crystals for low-energy elastic impacts [8-12], but the dynamic response of 2D and 3D granular crystals to higher-energy impacts and the effect of dissipation due to plastic deformations is just beginning to be investigated [13]. Recent work on

* Chiara Daraio. Tel.: +41 44 632 89 46.
E-mail address: daraio@ethz.ch.

Peer-review under responsibility of the Curators of the University of Missouri On behalf of the Missouri University of Science and Technology
doi:10.1016/j.proeng.2015.04.008

one-dimensional chains of metallic spheres subjected to an impact has shown that the addition of plasticity greatly affects the characteristics of stress waves travelling through materials [14-16]. This work applies recent findings on how materials properties determine the wave propagation properties of 1D elastic-plastic granular crystals to 2D and 3D systems. We then show a simple example of how the ability to control wave propagation speeds, dissipation and dispersion can be directly applied to guided wave mitigation for impact protection applications.

In order to take advantage of the unique wave propagation properties of elastic-plastic granular crystals, it is helpful to understand how they relate and compare to other systems of linear and non-linear granular materials. The plane wave propagation properties of lattices of point masses and linear springs are described by a dispersion relation that relates the frequency and wavelength of its normal modes [17]. The dispersion relation shows that the velocity at which excitations travel through these systems is proportional to $\sqrt{K/\rho}$ where K is the linear spring stiffness (N/m) and ρ is the mass density of the particle (kg/m^3), but is also dependent on the frequency. Because most impacts are composed of the superposition of waves of many frequencies, dispersion causes impact waves to spread based on their frequency content as they travel through a system of linear springs.

Lattices of granular matter, however, typically do not have linear contact interactions. When the particles are spherical and their contacts described by a Hertzian contact law, impacts create non-dispersive waves called solitons. The speeds at which solitons move through elastic granular crystals is not frequency dependent, but is dependent on the amplitude of the excitation [1]. For a fixed excitation amplitude, the speeds are no longer linearly proportional to $\sqrt{K/\rho}$ as in the elastic case. However, for 2D and 3D lattices of elastic particles with Hertzian contact interactions, Manjunath showed that predicted velocities of planar waves in 1D could be directly related to wave propagation through 2D and 3D lattices [11]. By using a scaling that took into account both the effects of stiffness changes due to contact geometry and density changes due to packing density, it was shown that:

$$V_{2D} = \frac{3}{2\sqrt{2}} V_{1D} \tag{1}$$

$$V_{3D} = \frac{2}{\sqrt{3}} V_{1D}, \tag{2}$$

where V here is travelling velocity of planar wave through Hertzian granular crystals of different dimensions.

In actual arrangements of metallic particles, stress concentrations at the contact points cause plasticity to occur even for relatively small impacts. Therefore the influence of plastic dissipation on the contact properties and on the properties of stress waves travelling through granular crystals of elastic-plastic particles is important for any impact protection application of these materials. Understanding the contact law that describes the force-displacement interaction between elastic-plastic particles allows us to simulate systems of particles using Discreet Element Methods (DEMs) [15,16,18]. The contact between elastic-plastic particles is initially Hertzian before the onset of yield. This is followed by a transition region as plasticity initiates until a final linear force-displacement state is reached. Simulations of 1D granular crystals of elastic-plastic particles have shown that because of their piece-wise non-linear contact law, they display a combination of the wave propagation properties of both linear and non-linear granular crystals. The initial non-linearity creates some amplitude dependence for the speed of stress wave propagation and causes stress waves to be non-dispersive and not frequency dependent. However, the initial wave speed is proportional to $\sqrt{K/\rho}$ where K is the stiffness in the linear regime, just as in the linear case [19]. In this work we extend previous work on 1D elastic-plastic granular systems to more complex 2D and 3D granular crystals using scaling approaches previously demonstrated for the elastic case. By understanding the dynamics in systems beyond model 1D materials, we can apply our approach and knowledge towards creating materials for real impact protection applications.

2. Numerical approach

A custom 3D DEM code was created in MATLAB using a contact law that models the force-displacement behavior of elastic-perfectly plastic spheres in dynamic compression to describe the interactions between point masses. At each time step, inter-particle forces are calculated and equations of motion are derived from Newton's second law. These coupled differential equations are then solved for each point mass in the system and advanced in time using a fixed time step, fourth-order Runge-Kutta method.

The contact law used was an experimentally verified model of the force versus displacement of elastic-perfectly plastic spheres in dynamic compression, which includes a description of strain-rate dependent materials [18]. The general form of the piece-wise, non-linear contact is given below:

$$F(\delta)=\begin{cases}(4/3)E^*\sqrt{r^*}\delta^{3/2} & \text{for } 0<\delta<\delta_y\\ \delta(\alpha+\beta\ln\delta) & \text{for } \delta_y<\delta<\delta_p\\ c_1\sigma_y\left(2r^*\delta+c_2\right) & \text{for } \delta>\delta_p,\end{cases} \tag{3}$$

where F is the contact force due to relative displacement between spherical particles δ. The effective Young's Modulus is $E^*=\left(\left(1-\upsilon_1^2\right)/E_1+\left(1-\upsilon_2^2\right)/E_2\right)^{-1}$ where E_1, E_2, ν_1 and ν_2 are the Young's Moduli and the Poisson's Ratio of the two materials and the effective radius as $r^*=(1/r_1+1/r_2)^{-1}$ where r_1 and r_2 are the radii of the two spheres. The first region ends at the onset of plasticity determined using the Von Mises criterion to be at a displacement δ_v and force F_y given by:

$$\delta_y=\frac{1}{4}\frac{r^*}{\left(E^*\right)^2}\left(1.6\sigma_y\pi\right)^2,\quad F_y=\frac{1}{6}\left(\frac{r^*}{E^*}\right)^2\left(1.6\sigma_y\pi\right)^3,$$

where in this study, σ_y is taken to be the minimum yield stress of the constituent materials. We are left with three empirical parameters that do not have analytical expressions: δ_p, c_1 and c_2, determined by Finite Element method fitting performed in Burgoyne 2014 [18]. All empirical parameters were determined through FEM simulations of 6.35 mm diameter hemispheres, but can be applied to other radii with appropriate scaling (with r in units of meters) is given by:

$$\delta_p=\left[0.0043\left(\frac{E^*}{\sigma_y}\right)^{-1}+1.47\times10^{-5}\right]\left(\frac{r^*}{0.00159}\right),\quad c_1=-6.76\left(\frac{E^*}{\sigma_y}\right)^{-0.137}+6.30,\quad c_2=\left[-3.99\times10^{-6}\left(\frac{E^*}{\sigma_y}\right)^{-1}+1.01\times10^{-9}\right]\left(\frac{r^*}{0.00159}\right)^2.$$

δ_p is the displacements at which the 2nd region ends and the force-displacement relation becomes linear corresponding to a force of $F_p=c_1\sigma_Y\left(2r^*\delta_P+c_2\right)$. α and β are solved to ensure continuity of the force between regions. This relation was formulated to describe the contact interaction between spheres of most metals and captures the behavior of the contact between two dissimilar spheres as well. Unloading was purely elastic with the formulation given by Wang [16].

A schematic of the elastic-plastic model is shown in blue in Figure 1a with the transitions between regions of the piece-wise function shown as dotted vertical lines at δ_y and δ_p. Figure 1a also shows the elastic Hertzian contact law in green. After unloading, subsequent reloading follows the Hertzian unloading curve back up until the previous maximum contact force has been reached and plastic deformation begin again. The history of plastic deformation at each contact point was therefore stored in a global variable and used to determine whether the current loading is elastic or plastic.

The first numerical setup in the work was used to model experiments performed in a drop weight test. Two layers of 3D hexagonally close packed (HCP) spheres of the materials used in experiments were simulated during an impact of a rigid massive surface. Interactions between particles and rigid boundaries have the same force-displacement relation as a particle interacting with an identical particle due to symmetry. Rigid flats were incorporated into the numerical system by defining a polygonal boundary, a mass and an initial velocity. The base was given no initial velocity and an infinite mass, forcing it to remain stationary throughout simulations, while the impacting tip was given the same mass and velocity as the experimental impactor. The force versus time applied to the impacting rigid tip was compared to the forces measured by the dynamic load cell in the impactor during the experiments. One quarter of the schematic of this numerical setup is shown in Figure 1b with the impacted region shaded green.

For investigations of wave propagation properties in 1D, 2D and 3D systems, the impacts on semi-infinite half spaces of model materials were simulated using periodic boundary conditions. In the 1D, 2D and 3D systems, 50 layers of close-packed particles were arranged in the z-direction. A schematic of the arrangements for 1D, 2D and 3D simulations is shown in Figure 1c. For 1D, a single chain of 50 particles was used. In the 2D and 3D systems, periodic boundary conditions were implemented into the numerical scheme by assigning particles on the boundary a periodic complement on the opposite boundary with which inter-particle forces were shared. The 2D simulations consisted of 50 hexagonally packed layers in the z-direction with five particles across the width in the direction of periodicity. The 3D simulations consisted of 50 layers of HCP spheres in the z-direction with hexagons of three particles per side in the plane of periodicity. No boundary conditions were applied to the bottom layer.

For these simulations, model materials were used with a variety of densities and yield stresses in order to investigate the material properties' effect on wave propagation. However, because the force is initially non-linear, there is some dependence on applied impulse [14]. Therefore, in each different case the loading was scaled based on the amplitude of the force required to reach the linear regime in the elastic-plastic model for that material. An impulse of magnitude $2F_p$ for the given material was applied to each particle in the top layer (a single particle for 1D, 5 particles for 2D, and 17 particles for 3D) for 100 x 10^{-6} seconds.

Local wave speeds after impacts were calculated by taking the arrival time of the wave to each layer divided by z-distance between subsequent layers. Arrival times at a given particle were taken to be when the particle's velocity reached

0.5% of its maximum velocity during the initial impact. Local wave speeds were nearly constant after some initial transient effects and were averaged over layers 5 through 25 to calculate local wave speed for each material for the $2F_p$ impulse.

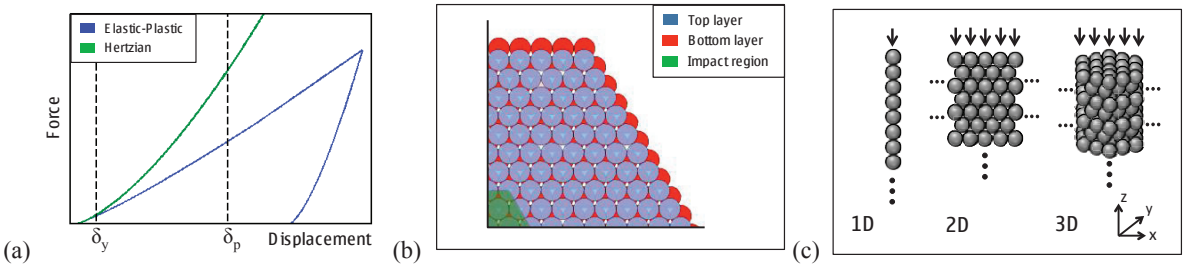

Fig. 1. (a) A plot of force versus displacement of the compression and unloading of two spherical particles. Blue shows the elastic-plastic model used in this work and green shows a purely elastic material described by the Hertzian contact law. (b) Schematic diagram showing a top down view of one quarter of the experimental arrangements of the spheres as well as the arrangement of particles for simulations of the experiment. Shaded green area (bottom left) is the impacted region. (c) A schematic of the numerical setup of spheres used for the analysis of stress wave speed in 1D, 2D and 3D materials. Black arrows show the direction in which the force is applied. All arrangements had 50 layers in the direction in which forces were applied. 2D and 3D simulations were performed with periodic boundary conditions on the sides.

3. Experimental methods

A drop weight tower at NASA Langley was used from heights of 0.46 m and 0.81 m to impact the granular crystals with impact velocities of 3 m/s and 4 m/s as measured directly above the sample with some variation due to friction losses during operation. The 2.3-kg impactor consisted of a cylindrical mass attached to an Instron Dynatup 90 kN load cell with flat tips made of hardened stainless steel 15-5. The weight of the impactor tips was minimized in order to reduce the internal vibrations measured by the load cell. The impactor tip section was hexagonal with side lengths of 12.7 mm in order to impact the selected area on the sample as shown in Figure 1b shaded in green color.

The materials used in experiments were 6.35 mm diameter spheres of Brass 260 and Stainless Steel 302 purchased from McMaster Carr. Their material properties are listed in Table 1 as given by the manufacturer. Foam board was used to contain the spheres such that all spheres would be in initial contact without providing any significant structural stiffness during the impact. The spheres were arranged on a large stainless steel 15-5 base which was rigid compared to softer spheres.

Table 1. Material properties used for simulations

Material	Density (units)	Young's modulus (units)	Yield strength (units)
Stainless steel 440	7650	200	1896
Stainless steel 302	7860	200	600
Aluminum 2017	2700	75	400
Brass 260	8530	110	670

4. Results and discussion

4.1. Experimental validation of numerical approach

In the numerical approach, it was assumed that the interactions between particles could be fully described by the normal force-displacement relationship. Friction can be ignored if either the tangential motion of the particles is negligible or if the magnitude of frictional forces is negligible compared to other forces on the particles. If friction were to play a significant role, it would contribute to additional stiffness by preventing particles from sliding past one another. Rotational motion of the spheres is also neglected. Angular motion can only be ignored if the energy lost to rotating the spheres is negligible compared to the energy lost due to plastic dissipation. Drop weight tower experiments were performed in order to investigate if our numerical approach can predict the behavior of elastic-plastic granular crystals given these assumptions or if any of these neglected effects play a role in the dynamics.

Figure 2 shows the comparison of experimental and numerical forces on the impactor for the two-layer HCP packing shown in Figure 1b, for both uniform brass and uniform stainless steel 302 systems. Despite only describing the normal interactions, the 3D DEM simulations predict correctly the magnitude of the forces and the impact duration, describing well the overall behavior of the system (e.g., the overall system's stiffness and energy transferred). From these results, we deduce that friction, tangential forces, and angular momentum play a secondary role in the dynamics of these systems. However, the experimental results typically show more oscillations after the peak force than predicted by the numerical simulations, this is likely a result of the mass of vibrations in the impactor.

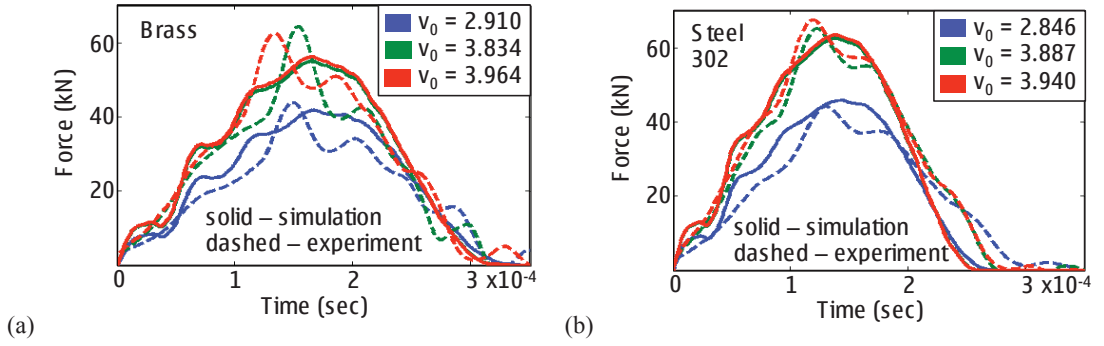

Fig. 2. Results from impacts performed on two-layer crystals of uniform materials. The plots compare the experimental and numerical forces on the impactor as a function of time (a) Impacts on arrangement of brass particles. (b) Impacts on arrangement of stainless steel 302 particles. Different initial velocities are shown in various colors, experimental data is shown with dashed lines while numerical predictions are shown as solid lines.

4.2. Determining stress wave speed

In periodic systems of masses and linear springs, waves travel at velocities determined by the stiffness of the springs and densities of the particles. In these systems the phase speed of acoustic waves is proportional to $\sqrt{K/\square}$. However the speed is also dependent on the frequency of the excitation as given by the dispersion relation of the material [17]. Non-linear systems like elastic granular crystals do not exhibit dispersion, but have wave speeds which are dependent on the amplitude of the excitation [1]. Because granular crystals with plasticity operate in both elastic and linear regimes, we observe a unique combination of wave propagation properties exhibited by both linear and Hertzian systems. In the one-dimensional case, it has been shown that while the wave speed in elastic-plastic systems is proportional to $\sqrt{K/\square}$ in the same manner as a linear system, it does not exhibit any dispersion. Furthermore, because the unique dynamics of elastic-plastic granular crystals is due to the dissipation of energy during plastic deformation, these properties only apply to the initial plastic wave. Subsequent reloading waves behave elastically like Hertzian granular crystals. However, there are many impact protection applications for which a single impact is to be expected or a second impact at the identical location is unlikely.

The wave speed of elastic-plastic granular crystals is somewhat amplitude dependent because the initial non-linearity determines how quickly the linear regime is reached. Therefore, in our numerical investigation the applied force on each particle in the first layer was always fixed such that $2F_p$, twice the required force to reach the linear region for that material, was initially experienced at each contact between the first and second layers. By fixing the relative initial contact force, the wave speeds' dependence on the material properties is decoupled from the amplitude dependence.

A parametric study was done by varying the density of the constituent material and the yield stress of a model material independently. In order to determine the dependence of the wave speed on the density of the particle material, simulations of impacts on 1D, 2D and 3D systems were performed with 10 densities between 2000 kg/m^3 and 16000 kg/m^3. For these simulations, the Young's modulus and yield stress were fixed at 100 GPa and 500 MPa respectively. The simulated speed of the stress wave travelling though the material was averaged over 20 layers for each density and each geometry and shown as markers in Figure 3a. By fitting curves to the numerical data we see that the wave speed of 2D and 3D elastic-plastic granular crystals continues to be inversely proportional to the square root of the density of the particle material. Furthermore, if we scale the fitting curves using Equations (1) and (2) based on the changes in stiffness and packing densities in the same manner demonstrated by Manjunath in the elastic case [11], all the fits collapse to a single curve. Therefore, despite the additional piece-wise non-linearities in the elastic-plastic case, the density dependence exhibited by 1D granular chains can still be scaled to 2D and 3D granular crystals.

Next, in order to determine the dependence of the wave speed on the stiffness of the contact between particles, simulations of impacts on 1D, 2D and 3D systems were performed with 10 yield stresses between 100 MPa and 2500 MPa.

In the linear region of the elastic-plastic model, the stiffness of the contact is mainly determined by the yield stress of the particle materials. For the 1D contact, the stiffness of the linear regime, K_{1D}, is given by [18]:

$$K_{1D} = 2\sqrt{r^*}\sigma_y\left[6.76\left(\frac{E^*}{\sigma_y}\right)^{0.14} + 6.30\right] \quad (4)$$

For these simulations, the Young's modulus and density were fixed at 100 GPa and 5000 kg/m^3 respectively. Therefore, using Equation (4), the range of yield stresses used corresponds to a range of stiffness from 3.5 x 10^6 N/m to 4.8 x 10^7 N/m. The simulated speed of the stress wave travelling though the material was averaged over 20 layers for each stiffness and each geometry and shown as markers in Figure 3b. By again fitting curves to the numerical data we see that the wave speed of 2D and 3D elastic-plastic granular crystals continues to be proportional to the square root of the 1D contact stiffness. Now if we again scale the fittings based on the geometrical correction factors in Equations (1) and (2), the parameter fittings all collapse to a single curve [11]. Just as with the density, the stiffness dependence exhibited by 1D granular chains can be easily scaled to 2D and 3D granular crystals.

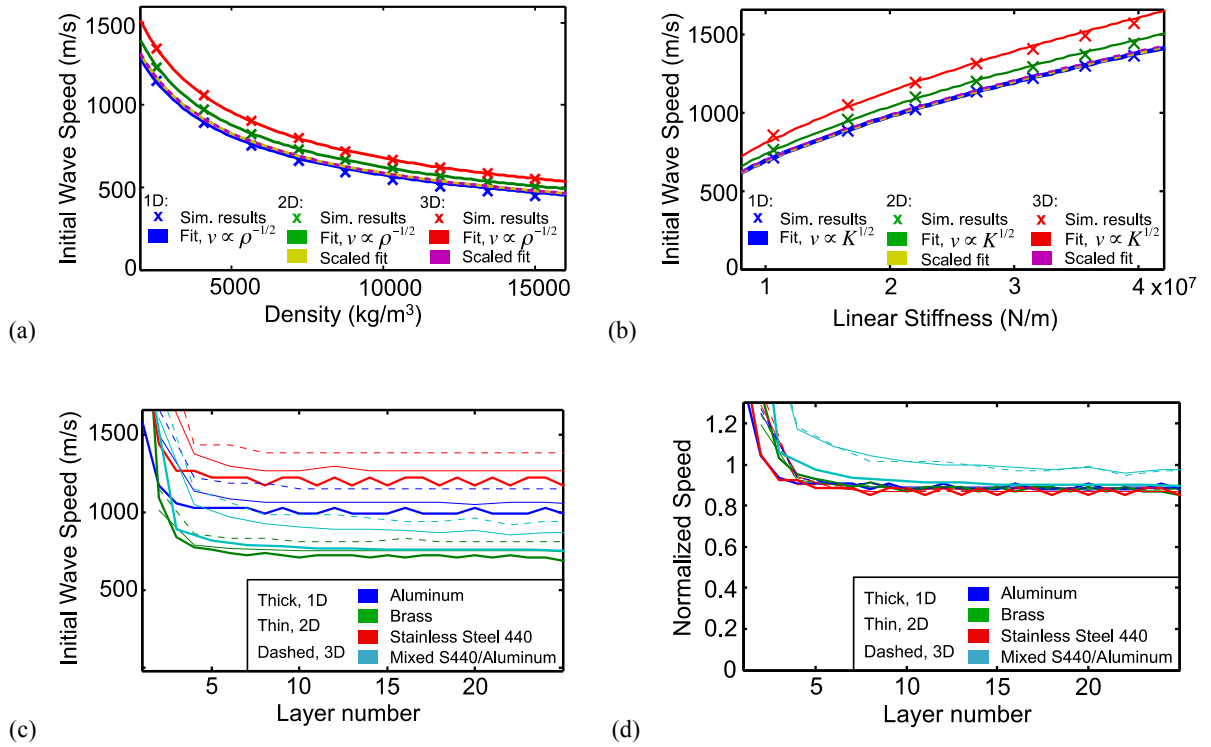

Fig. 3. (a) DEM results of a parametric study of initial stress wave speed versus the density of the material used in 1D, 2D and 3D close-packed arrangements of particles. Markers represent the wave speed observed in DEM simulations with solid lines showing the wave speed dependence on the square root of the inverse of density. Dashed lines (yellow and purple) show this fit scaled by the factor determined by the geometry and are nearly indistinguishable and overlap with 1D results (blue). (b) DEM results of a parametric study of initial stress wave speed versus the stiffness of the material used in 1D, 2D and 3D close-packed arrangements of particles. Markers represent the wave speed observed in DEM simulations with solid lines showing the wave speed dependence on the square root of the stiffness. Dashed lines show this fit scaled by the factor determined by the geometry. (c) Plots of the simulated local speed of the wave as it travel through 1D, 2D and 3D arrangements of particles of real materials. (d) Plots of the simulated local speed of the wave as it travel through 1D, 2D and 3D arrangements of particles of real materials normalized by the dependence on the stiffness, density, and the geometry.

As shown in the 1D case, knowing how the wave speed scales with the density and yield stress of the constituent materials, allows us to predict the stress wave propagation properties of new combinations of materials [19]. We have now shown that this approach can be scaled to close packed 2D and 3D granular crystals and allow us to predict the properties of increasingly complex systems of real materials. The predicted wave speeds through each layer in 1D, 2D and 3D granular crystals of four real materials are shown in Figure 3c. If we then take these wave speeds and normalize them both by

materials properties and geometry according to Equations (1) and (2), we can define the following normalized wave velocities:

$$V_{\text{norm}} = V \Big/ \left(A \sqrt{\frac{K_{1D}}{R \rho_{1D}}} \right) \qquad \text{where } A = \begin{cases} \dfrac{3}{2\sqrt{2}} & \text{for 2D} \\ \dfrac{2}{\sqrt{3}} & \text{for 3D} \end{cases} \tag{5}$$

where R is the radius of the spheres. The results of this scaling for the real materials used are shown in Figure 3d. We see that all systems comprised of just one material collapse to a single curve. Therefore, by knowing the density of the constituent material and using Equation (4) to get the linear stiffness of the 1D contact, we can predict the initial wave velocity of 1D, 2D and 3D close-packed, elastic-plastic granular crystals. It has been previously shown the normalization is also valid for 1D granular crystals with alternating materials [19]. Interestingly, 2D and 3D granular crystals with alternating layers of 2 materials appear to have a slightly different normalized wave speed. This is perhaps due to a new deformation mechanism between hard and soft layers that violate the quasi-one dimensional nature of the previous periodic simulations, i.e., soft particles being pushed aside by harder particles and moving in other dimensions which don't exist in 1D. More detailed simulations will be performed to investigate this effect.

4.3. Guided impact applications

We have shown that speed of stress waves due to impacts in elastic-plastic granular crystals is determined by the materials properties of the local constituent particles. Because granular systems give us the freedom to choose the materials properties of each individual particle we can create highly anisotropic materials with designed geometries. Using our understanding of the wave propagation properties in elastic-plastic granular crystals, we can create metamaterials with designed responses to various impacts.

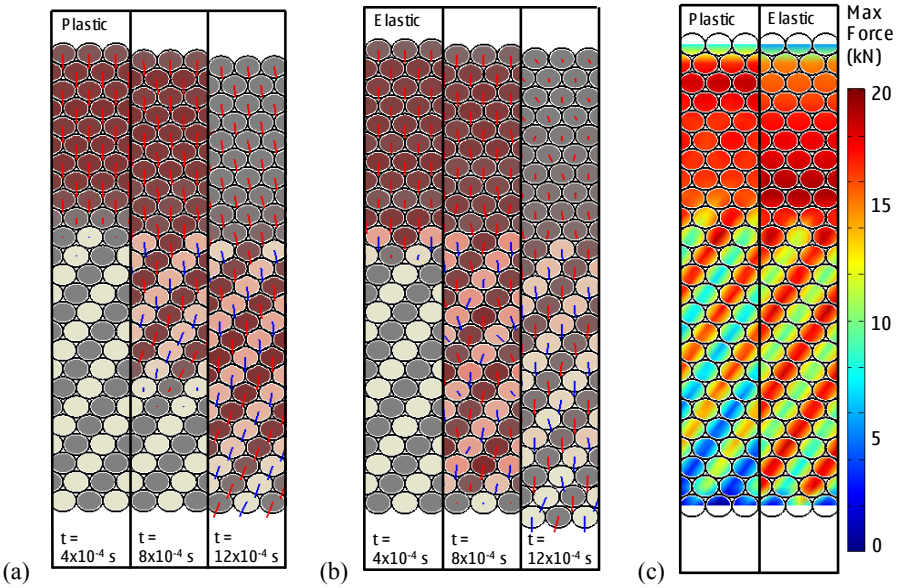

Fig. 4. (a), (b) Depictions of the location, velocity and force on each particle at different times following an impact on a system (a) with plasticity and (b) assuming only elastic (Hertzian) interactions between particles. Initial color represents the particle material with dark particles being stainless steel 440 and light particles being aluminum. Red color depicts force on the particle relative to the maximum forces experienced during the impact. Red and blue lines show the direction of the velocity of steel and aluminum particles respectively with the length of the line normalized by the maximum velocity in any of the particles at that time step. (c) Depiction of the maximum force felt by each particle during the impact for both contact laws.

An example is shown in Figure 4 where arrangements of stainless steel 440c and aluminum are used to create a change in the direction of particle velocities within a material. An initial impulse of $2F_p$ for the stainless steel 440c was applied to 25 layers of hexagonally close packed spheres which are 15 particles wide in the periodic direction. After 10 layers of stainless steel 440c, we introduced stripes of alternating aluminum and stainless steel 440c at a 30-degree angle from the initial pulse.

In Figure 4a, we see that as the wave entered into the striped region, after a few layers of transition, the particle velocities aligned with the stripes and traveled at 30-degree from the initial wave direction. However, when only elastic interactions were assumed, the new geometry created some local changes in direction of the particle velocities, but the wave generally continued in the z-direction as seen in Figure 4b. Because the elastic-plastic particle systems allow us to control the local particle velocity, we can design materials with anisotropic and inhomogeneous wave propagation properties where impacts can be directed away from sensitive areas of materials and towards less sensitive areas. In Figure 4c we can also see that, in the elastic-plastic case, forces were dissipated within the material due to permanent plastic deformations and the maximum forces were lower in each subsequent layer of material.

5. Summary and future work

In this work we have computationally and experimentally investigated the relations between dynamics of 1D, 2D and 3D elastic-plastic granular crystals. First we showed that we could capture the behavior of elastic-plastic 3D granular crystals with DEM simulations using only the normal contact law to describe interactions between particles. We then determined how the properties of waves travelling in these materials depend on the material properties of the constituent particles. We showed that the properties of 1D chains of elastic-plastic particles can be applied to 2D and 3D systems using a geometric scaling previously used to analyze elastic systems. With the new understanding of wave propagation properties in elastic-plastic granular crystals, we showed an unoptimized example of how geometry and choice of materials can lead to novel protection systems. By creating materials with unique anisotropic wave propagation properties we can direct impacts within materials in order to influence which parts within a material experience the effect of an impact.

Our next goal is to explore further geometries including determining the influence of oblique impacts and impacts on different crystal orientations. The example given of an anisotropic material used for impact protection can be optimized for both geometry and materials used. We can better characterize these materials' ability to protect from different types of impacts through further simulations as well as more drop tower experiments including experiments with much higher impact velocities.

Acknowledgements

This research was supported by NASA Space Technology Research Fellowship (NSTRF) grant number NNX13AL66H as well as Air Force Office of Scientific Research (AFOSR) grant number FA9550-12-1-0091 through the University Center of Excellence in High-Rate Deformation Physics of Heterogeneous Materials.

References

[1] Nesterenko, V., Dynamics of Heterogeneous Materials. 2001, New York: Springer New York.
[2] Leonard, A.; Chong, C.;Kevrekidis, P.G.; Daraio, C. Traveling waves in 2D hexagonal granular crystal lattices, Granular Matter, 2014. 16: p.531-542.
[3] Awasthi, A.P., et al., Propagation of solitary waves in 2D granular media: A numerical study. Mechanics of Materials, 2012. 54: p. 100-112.
[4] Chang, C.S., Gao, J., Non-linear dispersion of plane wave in granular media. International Journal of Non-Linear Mechanics, 1995. 30(2): p. 111-128.
[5] Leonard, A., Daraio, C., Stress Wave Anisotropy in Centered Square Highly Nonlinear Granular Systems. Physical Review Letters, 2012. 108(21).
[6] Leonard, A., Fraternali, F., Daraio, C., Directional Wave Propagation in a Highly Nonlinear Square Packing of Spheres. Experimental Mechanics, 2011. 53(3): p. 327-337.
[7] Mueggenburg, N., Jaeger, H., Nagel, S., Stress transmission through three-dimensional ordered granular arrays. Physical Review E, 2002. 66(3).
[8] Anfosso, J., Gibiat, V., Elastic wave propagation in a three-dimensional periodic granular medium. Europhysics Letters (EPL), 2004. 67(3): p. 376-382.
[9] Bourrier, F., F. Nicot, Darve, F., Physical processes within a 2D granular layer during an impact. Granular Matter, 2008. 10(6): p. 415-437.
[10] Manjunath, M., Awasthi, A.P., Geubelle, P.H., Wave propagation in 2D random granular media. Physica D: Nonlinear Phenomena, 2014. 266: p. 42-48.
[11] Manjunath, M., Awasthi, A.P., Geubelle, P.H., Plane wave propagation in 2D and 3D monodisperse periodic granular media. Granular Matter, 2014. 16(1): p. 141-150.
[12] Nishida, M., Tanaka, Y. , DEM simulations and experiments for projectile impacting two-dimensional particle packings including dissimilar material layers. Granular Matter, 2010. 12(4): p. 357-368.
[13] Pal, R.K., Geubelle, P.H., Impact response of elasto-plastic granular and continuum media: A comparative study. Mechanics of Materials, 2014. 73: p.38-50
[14] Pal, R.K., Awasthi, A.P., Geubelle, P.H., Wave propagation in elasto-plastic granular systems. Granular Matter, 2013. 15: p 747-758
[15] Pal, R.K., Awasthi, A.P., Geubelle, P.H., Characterization of wave propagation in elastic and elastoplastic granular chains, Physical Review E
[16] Wang, E., On. T., Lambros, J. An Experimental Study of the Dynamic Elasto-Plastic Contact Behavior of Dimer Metallic Granules. Journal of Applied Mechanics. 53: p. 883-892.
[17] Ashcroft, N.W., Mermin, N.D., Solid State Physics. 1976, Orlando: Saunders College Publishing.
[18] Burgoyne, H.A., Daraio, C., Strain-rate-dependent model for the dynamic compression of elastoplastic spheres. Physical Review E, 2014. 89(3).
[19] Burgoyne, H.A., Daraio, C. Manuscript in progress.